Macromolecules

Article

Novel Anodic Polyelectrochromic Aromatic Polyamides Containing Pendent Dimethyltriphenylamine Moieties

Cha-Wen Chang, Chen-Hsien Chung, and Guey-Sheng Liou

Macromolecules, **2008**, 41 (22), 8441-8451 • Publication Date (Web): 22 October 2008

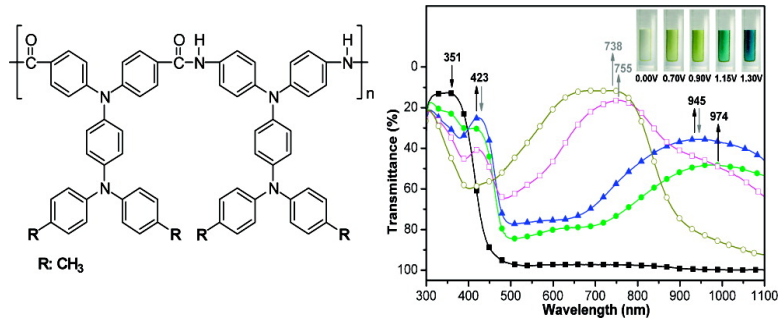

More About This Article

Additional resources and features associated with this article are available within the HTML version:

- Supporting Information
- Access to high resolution figures
- Links to articles and content related to this article
- Copyright permission to reproduce figures and/or text from this article

View the Full Text HTML

Novel Anodic Polyelectrochromic Aromatic Polyamides Containing Pendent Dimethyltriphenylamine Moieties

Cha-Wen Chang,[†] Chen-Hsien Chung,[†] and Guey-Sheng Liou*[,‡]

Department of Applied Chemistry, National Chi Nan University, 1 University Road, Puli, Nantou Hsien 54561, Taiwan, Republic of China, Institute of Polymer Science and Engineering, National Taiwan University, Taipei, 10617, Taiwan, Republic of China

Received June 2, 2008; Revised Manuscript Received August 22, 2008

ABSTRACT: Two series of novel aromatic polyamides containing pendent dimethyltriphenylamine moieties were prepared based on *N*,*N*-bis(4-aminophenyl)-*N*′,*N*′-di(4-methylphenyl)-1,4-phenylenediamine (**4**) and *N*,*N*-bis(4-carboxyphenyl)-*N*′,*N*′-di(4-methylphenyl)-1,4-phenylenediamine (**4**′). These compounds with similar structures were successfully synthesized by amination reactions of 4-amino-4′,4″-dimethyltriphenylamine with 4-fluoronitrobenzene and 4-fluorobenzonitrile, respectively; subsequent reduction and alkaline hydrolysis of the dinitro and dinitrile intermediates led to new triphenylamine-containing aromatic diamine and dicarboxylic acid monomers. These polyamides, with pendent 4,4′-dimethyl-substituted triphenylamine (TPA) units having inherent viscosities of 0.34−0.80 dL/g, were prepared via direct phosphorylation polycondensation. All the polymers were amorphous with good solubility in many organic solvents, such as *N*-methyl-2-pyrrolidinone (NMP) and *N*,*N*-dimethylacetamide (DMAc), and could be solution-cast into tough and flexible polymer films. These aromatic polyamides had useful levels of thermal stability associated with their relatively high glass transition temperature (236−288 °C), 10% weight-loss temperatures in excess of 505 °C, and char yields at 800 °C in nitrogen higher than 68%. The electrochromic properties are examined by electrochemical and spectroelectrochemical methods. Cyclic voltammograms of polyamide **IIc**, prepared from the dicarboxylic acid monomer **4**′ with the structurally similar diamine monomer **4**, exhibited four reversible oxidation redox couples in acetonitrile solution at $E_{1/2}$ = 0.58, 0.76, 0.96, and 1.12 V, respectively. All the polyamides exhibited excellent reversibility of electrochromic characteristics by continuous five cyclic scans between 0.0 to 1.30 V, with a color change from the original pale yellowish neutral form to the green and then to blue oxidized forms. Polyamide **Ib** not only showed excellent reversible electrochromic stability with good coloration efficiency of green (CE = 276 cm^2/C) but also exhibited high contrast of optical transmittance change (ΔT, %) up to 52% at 423 nm and 67% at 1003 nm for green. After over 1600 cyclic switches, the polymer films still exhibited excellent stability of electrochromic characteristics.

Introduction

Electrochromism can be defined as the reversible change in optical properties of a material resulting from electrochemically induced redox states. Electrochromic materials that exhibit several colors are termed polyelectrochromic.[1] This interesting property led to the development of many technological applications such as display panels,[2] camouflage materials,[3] variable-reflectance mirrors,[4] and variable-transmittance windows.[5] Conducting or conjugated polymers have been found to be more promising as electrochromic materials because of their better stability, faster switching speeds, and easy processing compared to inorganic electrochromic materials, but the most exciting properties are multiple colors for the same material while switching between different redox states[6] and fine-tuning of the color transition through chemical structure modification of the conjugated backbone.[7,8]

Anodic electrochromic materials are those that exhibit multiple colors depending upon their oxidation states. One of the most interesting multicolor systems is that based upon the *N*,*N*,*N*′,*N*′-tetraphenyl-*p*-phenylenediamine moiety.[9] Intramolecular electron transfer and electronic coupling effects in the oxidized states are important in the design of new *N*,*N*,*N*′,*N*′-tetraphenyl-*p*-phenylenediamine-based polymers for electrochromic devices. Intramolecular electron transfer (ET) processes have been studied extensively in the mixed-valence (MV) systems.[10−12] They usually employed one-dimensional MV compounds containing two or more redox states connected via σ- or π-bridge molecule. According to Robin and Day,[13] an experimental and theoretical study of the *N*,*N*,*N*′,*N*′-tetraphenyl-*p*-phenylenediamine cation radical has been reported and a symmetrical delocalized class III structure with strong electronic coupling (with the electron delocalized over the two redox centers) was proposed.[14]

In order to be useful for applications, electrochromic materials must exhibit long-term stability, multiple colors with the same material, and large changes in transmittance (large ΔT, %) between their bleached and colored states.[15] Our strategy was to synthesize the *N*,*N*,*N*′,*N*′-tetrasubstituted-1,4-phenylenediamine monomers such as diamines and dicarboxylic acids that phenyl groups were incorporated by electron-donating substituents at the para position of triphenylamine (TPA), the coupling reactions were greatly prevented by affording stable cationic radicals and lowering the oxidation potentials.[9] The corresponding polymers with high molecular weights and high thermal stability could be obtained through conventional polycondensation techniques. Because of the incorporation of packing-disruptive, propeller-shaped TPA units along the polymer backbone, most of these polymers exhibited good solubility in polar organic solvents, and uniform, transparent amorphous thin films could be obtained by solution casting and spin-coating methods. This is advantageous for ready fabrication of large-area, thin-film devices.

In this paper, we therefore synthesized a new, structurally similar diamine, *N*,*N*-bis(4-aminophenyl)-*N*′,*N*′-di(4-methylphenyl)-1,4-phenylenediamine (**4**), and diacid, *N*,*N*-bis(4-carboxyphenyl)-*N*′,*N*′-di(4-methylphenyl)-1,4-phenylenediamine (**4**′), and their derived polyamides containing one or two *N*,*N*,*N*′,*N*′-tetraphenyl-*p*-phenylene units that have multiple redox potentials

* Corresponding author: e-mail gsliou@ntu.edu.tw.
[†] National Chi Nan University.
[‡] National Taiwan University.

10.1021/ma801227j CCC: $40.75
Published on Web 10/22/2008

Scheme 1. Synthesis of Monomers

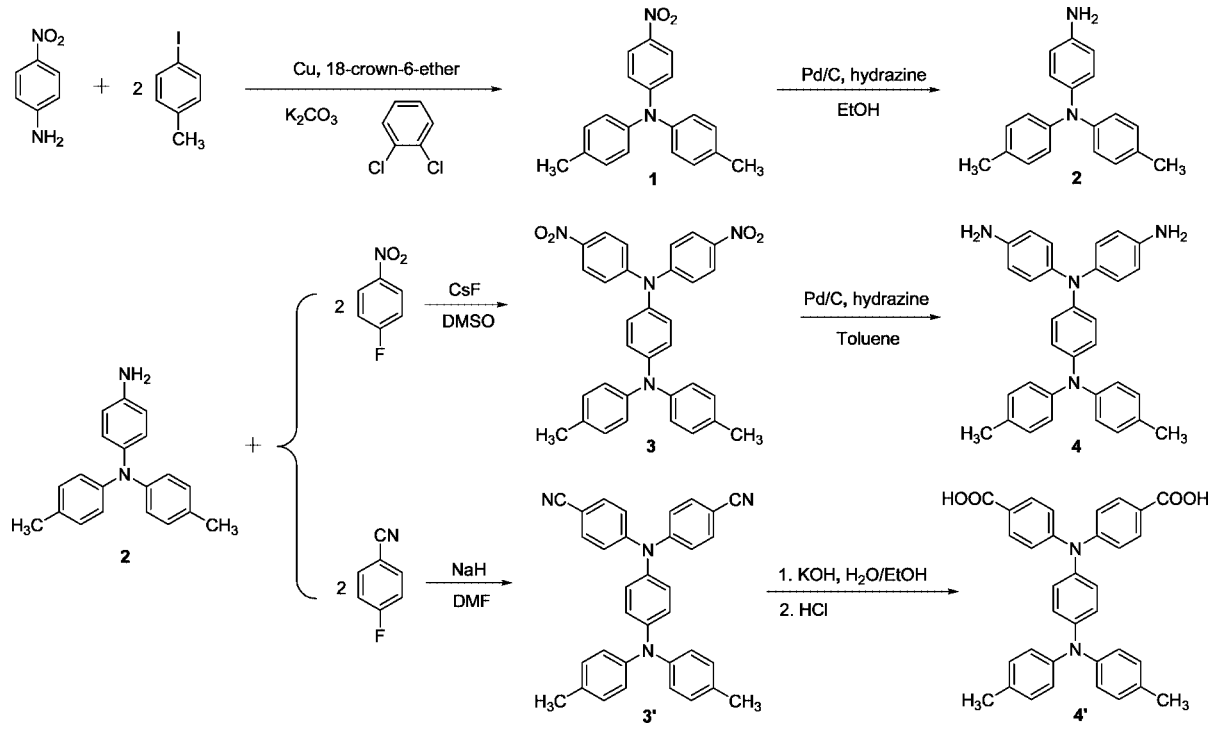

to produce multiple colors. General properties such as solubility and thermal properties are described. Electrochemical and electrochromic properties of these polymers are also described herein and are compared with those of structurally related polymers from *N*,*N*-bis(4-aminophenyl)-*N*′,*N*′-diphenyl-1,4-phenylenediamine.[16]

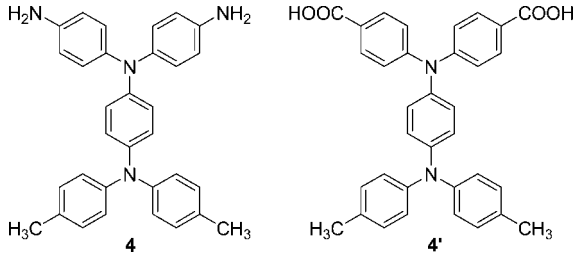

Experimental Section

Materials. *N*,*N*-Bis(4-aminophenyl)-*N*′,*N*′-diphenyl-1,4-phenylenediamine (mp = 245−247 °C) was synthesized by hydrazine Pd/C-catalyzed reduction of *N*,*N*-bis(4-nitrophenyl)-*N*′,*N*′-diphenyl-1,4-phenylenediamine resulting from the condensation of 4-aminotriphenylamine with 4-fluoronitrobezene in the presence of cesium fluoride (CsF) according to a previously reported procedure.[17] 4-Iodotoluene (Acros), 4-nitroaniline (Acros), 4-fluoronitrobenzene (Aldrich), 4-fluorobenzonitrile (TCI), potassuim carbonate (Acros), copper powder (Acros), 18-crown-6 ether (TCI), sodium hydride (95%, dry, Aldrich), *o*-dichlorobenzene (Tedia), *N*,*N*-dimethylacetamide (DMAc) (Tedia), *N*,*N*-dimethylformamide (DMF) (Acros), dimethyl sulfoxide (DMSO) (Tedia), *N*-methyl-2-pyrrolidinone (NMP) (Tedia), pyridine (Py) (Tedia), and triphenyl phosphite (TPP) (Acros) were used without further purification. Commercially available aromatic dicarboxylic acids and diamines such as terephthalic acid (**5a**), 4,4′-oxybis(benzoic acid) (**5b**), 2,2-bis(4-carboxyphenyl)hexafluoropropane (**5c**), *p*-phenylenediamine (**5′a**), and 4,4′-oxybis(aniline) (**5′b**) were purchased from TCI and used as received. Commercially obtained anhydrous calcium chloride ($CaCl_2$) was dried under vacuum at 180 °C for 8 h. Tetrabutylammonium perchlorate (TBAP) (Acros) was recrystallized twice by ethyl acetate under nitrogen atmosphere and then dried in vacuo prior to use. All other reagents were used as received from commercial sources.

Monomer Synthesis: 4-Nitro-4′,4″-dimethyltriphenylamine (1). According to known chemistry,[18] compound **1** (yield 66%, mp 168−170 °C) was prepared by potassium carbonate-mediated aromatic nucleophilic substitution reaction of 4-nitroaniline with 4-iodotoluene.

4-Amino-4′,4″-dimethyltriphenylamine (2). In a 250-mL three-neck round-bottom flask equipped with a stirring bar under nitrogen atmosphere, 7.26 g (22.80 mmol) of nitro compound (**1**) and 0.20 g of 10% Pd/C were dissolved/suspended in 50 mL of ethanol. The suspension solution was heated to reflux, and 5 mL of hydrazine monohydrate was added slowly to the mixture; then the solution was stirred at reflux temperature. After a further 9 h of reflux, the solution was filtered to remove Pd/C, and the filtrate was cooled to precipitate. The product was collected by filtration and dried in vacuo at 80 °C to give 5.26 g (80% in yield) of off-white crystals: mp 114−116 °C measured by DSC at 10 °C/min; IR (KBr) 3436, 3358 cm^{-1} (N−H stretch), 2919 cm^{-1} (CH_3 C−H stretch); ^1H NMR (300 MHz, $CHCl_3$-*d*, δ, ppm) 2.19 (s, 6H, CH_3), 4.99 (s, 2H, NH_2), 6.53 (d, 2H, H_a), 6.73 (d, 2H, H_b), 6.76 (d, 4H, H_c), 6.98 (d, 4H, H_d); ^{13}C NMR (75 MHz, $CHCl_3$-*d*, δ, ppm) 20.5 (CH_3), 115.4 (C^2), 121.9 (C^6), 127.6 (C^3), 129.8 (C^7), 130.1 (C^8), 136.4 (C^4), 145.6 (C^1), 146.1 (C^5). Anal. Calcd for $C_{20}H_{20}N_2$ (288.38): C, 83.30; H, 6.99; N, 9.71. Found: C, 82.99; H, 7.02; N, 9.56.

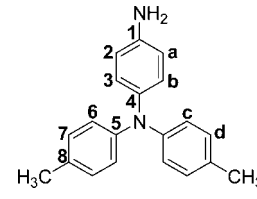

***N*,*N*-Bis(4-nitrophenyl)-*N*′,*N*′-di(4-methylphenyl)-1,4-phenylenediamine (3).** A mixture of 3.71 g (24.40 mmol) of cesium fluoride in 35 mL of dimethyl sulfoxide (DMSO) was stirred at room temperature. To the mixture were added, in sequence, 3.06 g (10.61 mmol) of **2** and 3.14 g (22.28 mmol) of 4-fluoronitrobenzene. The mixture was heated with stirring at 120 °C for 24 h. The mixture was poured into

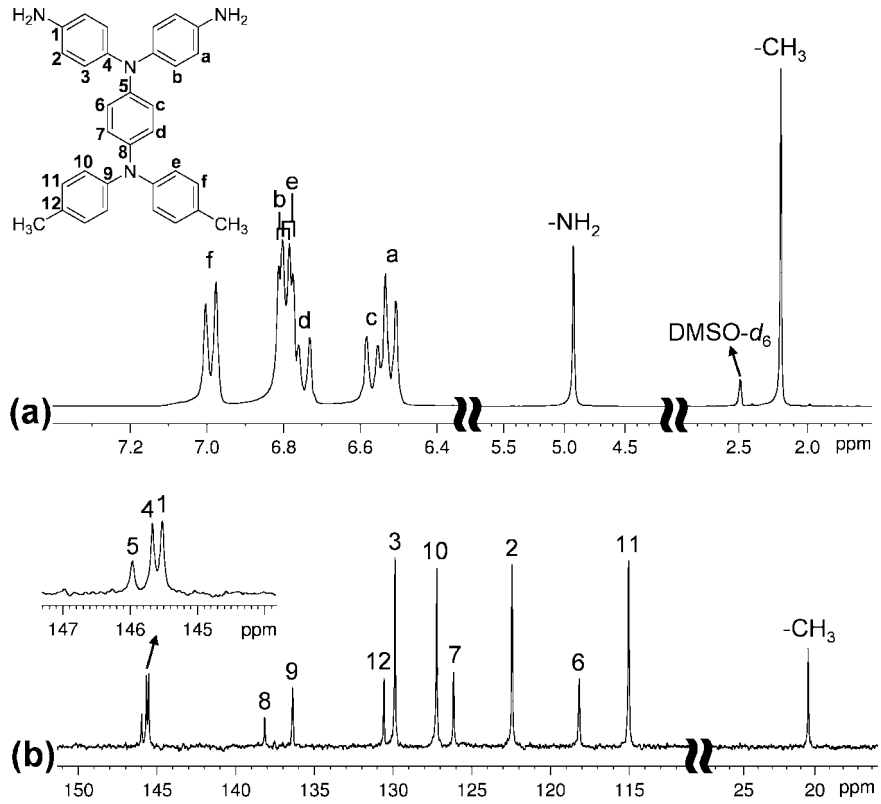

Figure 1. (a) ^{1}H NMR and (b) ^{13}C NMR spectra of compound **4** in DMSO-d_6.

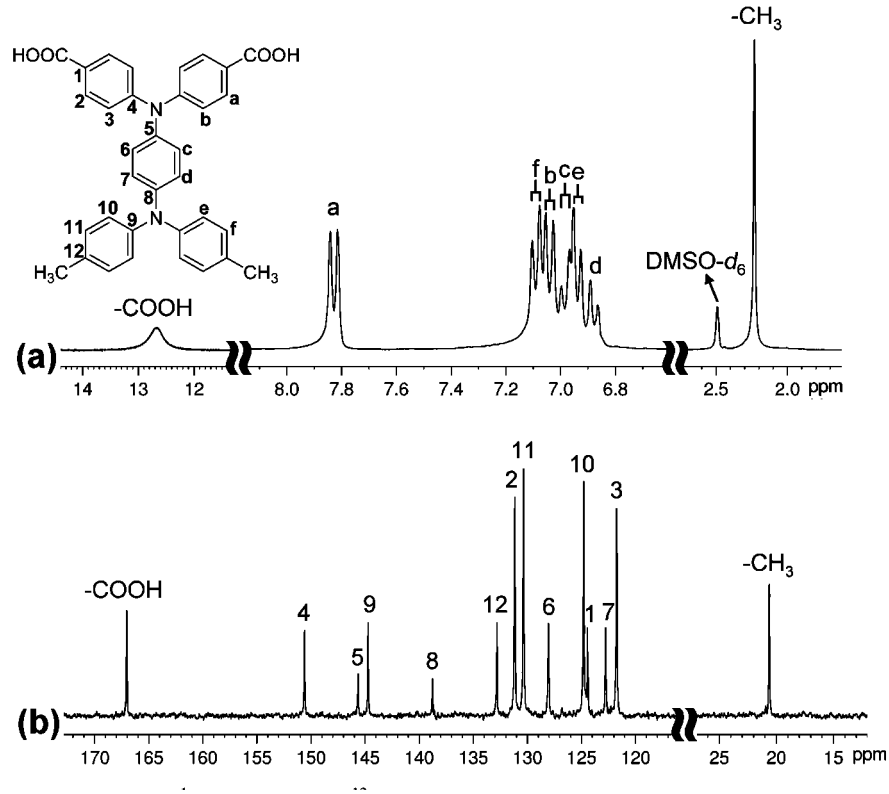

Figure 2. (a) ^{1}H NMR and (b) ^{13}C NMR spectra of compound **4′** in DMSO-d_6.

200 mL of stirred water slowly, and the precipitated red powder was collected by filtration and washed thoroughly with methanol/acetonitrile. The product was filtered to afford 3.94 g (70% in yield) of red powder: mp 298−300 °C measured by DSC at 10 °C/min; IR (KBr) 2915 cm^{-1} (CH_3 C−H stretch), 1580, 1343 cm^{-1} (NO_2 stretch); ^{1}H NMR (300 MHz, $CDCl_3$-*d*, δ, ppm) 2.33 (s, 6H, CH_3), 6.93 (d, 2H, H_d), 7.00 (d, 2H, H_c), 7.05 (d, 4H, H_f), 7.11 (d, 4H, H_e), 7.17 (d, 4H, H_b), 8.14 (d, 4H, H_a); ^{13}C NMR (75 MHz, $CDCl_3$-*d*, δ, ppm) 20.9 (CH_3), 121.8 (C^3), 122.2 (C^6), 125.3 (C^{10}), 125.5 (C^2), 128.0 (C^7), 130.2 (C^{11}), 133.7 (C^{12}), 136.8 (C^8), 142.4 (C^9), 144.5 (C^1), 147.4 (C^5), 151.9

Scheme 2. Synthesis of Polyamides by Direct Polycondensation Reaction

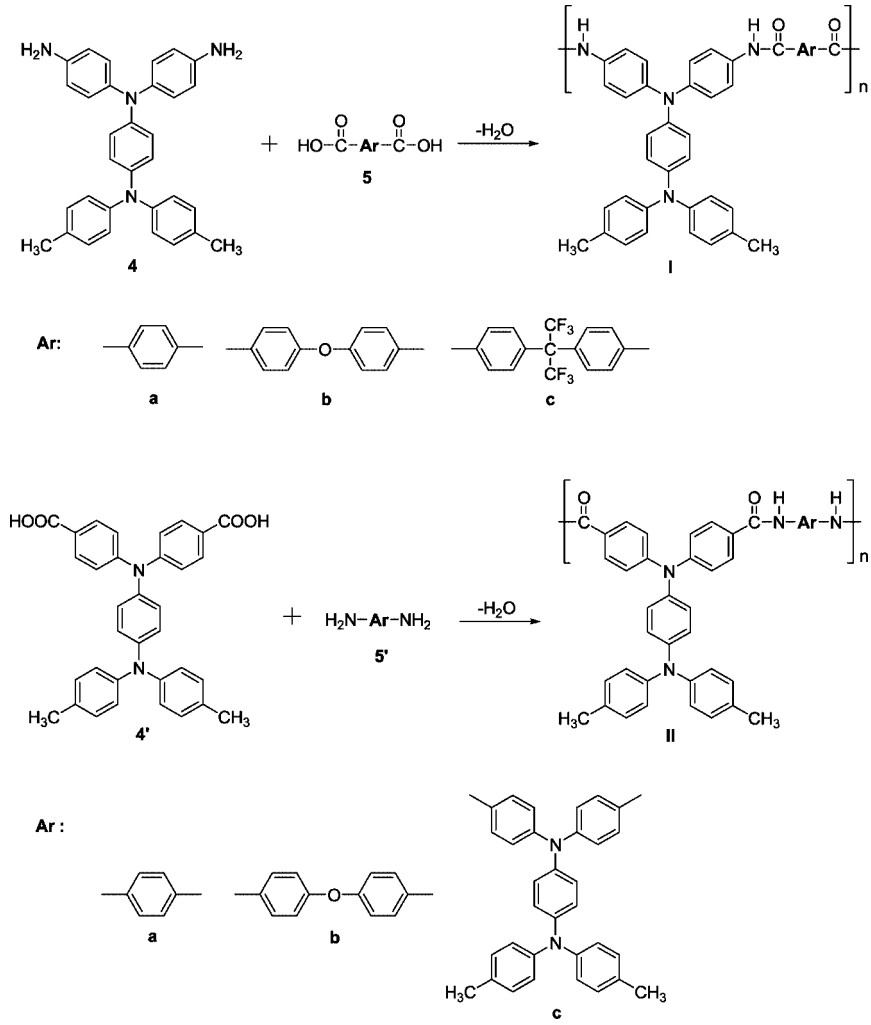

Table 1. Inherent Viscosities and Solubility of Polyamides

			solvent[b]						
polymer	η_{inh}[a] (dL/g)	yield (%)	NMP	DMAc	DMF	*m*-cresol	THF	$CHCl_3$	MeOH
Ia	0.60	99	++	++	++	++	−	−	−
Ib	0.80	99	++	++	++	++	−	−	−
Ic	0.34	98	++	++	++	++	±	−	−
IIa	0.65	99	++	+	+	±	−	−	−
IIb	0.54	99	++	++	±	±	−	−	−
IIc	0.48	98	++	++	+	±	±	±	−

[a] Measured at a polymer concentration of 0.5 g/dL in NMP at 30 °C. [b] Qualitative solubility was tested with 1 mg of sample in 1 mL of stirred solvent: ++, soluble at room temperature; +, soluble on heating; ±, partially soluble; −, insoluble even on heating.

(C^4). Anal. Calcd for $C_{32}H_{26}N_4O_4$ (530.57): C, 72.44; H, 4.94; N, 10.56. Found: C, 72.38; H, 4.86; N, 10.71.

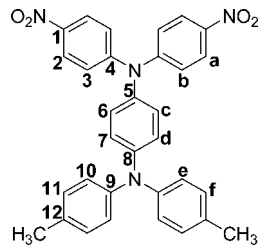

***N*,*N*-Bis(4-aminophenyl)-*N'*,*N'*-di(4-methylphenyl)-1,4-phenylenediamine (4).** In a 250-mL three-neck round-bottom flask equipped with a stirring bar under nitrogen atmosphere, 1.00 g (1.88 mmol) of nitro compound **3** and 0.02 g of 10% Pd/C were dissolved/suspended in 58 mL of toluene. The suspension solution was heated at 75 °C, and 1 mL of hydrazine monohydrate was added slowly to the mixture; then the solution was stirred at 85 °C. After a further 12 h of reaction, the solution was filtered to remove Pd/C, and the filtrate was cooled to precipitate. The product was collected by filtration and dried in vacuo at 100 °C to give 0.75 g (85% in yield) of olivine crystal: mp 277−279 °C measured by DSC at 10 °C/min; IR (KBr) 3456, 3366 cm^{-1} (N−H stretch), 2920 cm^{-1} (CH_3 C−H stretch); ^{1}H NMR (300 MHz, DMSO-d_6, δ, ppm) 2.19 (s, 6H, CH_3), 4.93 (s, 4H, NH_2), 6.52 (d, 4H, H_a), 6.57 (d, 2H, H_c), 6.75 (d, 2H, H_d), 6.79 (d, 4H, H_e), 6.80 (d, 4H, H_b), 6.99 (d, 4H, H_f); ^{13}C NMR (75 MHz, DMSO-d_6, δ, ppm) 20.5 (CH_3), 115.0 (C^{11}), 118.2 (C^6), 122.4 (C^2), 126.2 (C^7), 127.2 (C^{10}), 129.9 (C^3), 130.6 (C^{12}), 136.4 (C^9), 138.1 (C^8), 145.5 (C^1), 145.7 (C^4), 146.0 (C^5). Anal. Calcd for $C_{32}H_{30}N_4$ (470.60): C, 81.67; H, 6.43; N, 11.91. Found: C, 81.29; H, 6.39; N, 11.69.

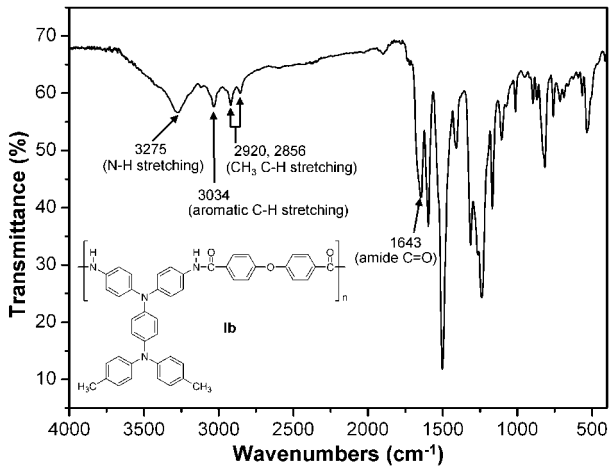

Figure 3. IR spectrum of polyamide **Ib** film.

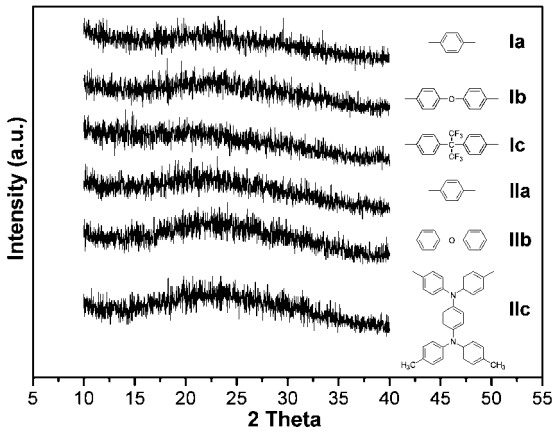

Figure 4. WAXD patterns of polyamide films.

Table 2. Thermal Properties of Polyamides

polymer	T_g[a] (°C)	T_s[b] (°C)	T_d at 5% weight loss[c] (°C)		T_d at 10% weight loss[c] (°C)		char yield[d] (wt %)
			N_2	air	N_2	air	N_2
Ia	279	275	495	480	555	530	74
Ib	262	263	505	490	555	540	73
Ic	288	302	505	505	550	545	70
IIa	280	268	480	450	550	505	73
IIb	244	244	475	450	540	510	68
IIc	236	235	470	450	540	510	72

[a] Midpoint temperature of the baseline shift on the second DSC heating trace (rate = 20 °C/min) of the sample after quenching from 400 to 50 °C (rate = 200 °C/min) in nitrogen. [b] Softening temperature measured by TMA with a constant applied load of 50 mN at a heating rate of 10 °C/min. [c] Decomposition temperature, recorded via TGA at a heating rate of 20 °C/min and a gas-flow rate of 30 cm^3/min. [d] Residual weight percentage at 800 °C in nitrogen.

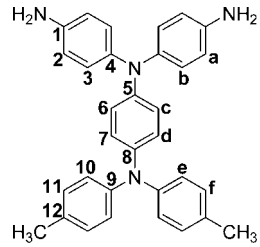

***N,N*-Bis(4-cyanophenyl)-*N′,N′*-di(4-methylphenyl)-1,4-phenylenediamine (3′).** A mixture of 0.65 g (27 mmol) of sodium hydride and 50 mL of DMF was stirred at room temperature under nitrogen for 30 min, and then 3.46 g (12 mmol) of compound **2** was added. After the evolution of hydrogen was complete, 3.05 g (25.2 mmol) of 4-fluorobenzonitrile were added in sequence. The mixture was heated with stirring at 140 °C for 10 h and then precipitated into 300 mL of methanol and 400 mL of water. The products was filtered and recrystallized from acetone to give 1.47 g (24% yield) of yellowish needles: mp 261−262 °C measured by DSC at 10 °C/min; IR (KBr) 2915 cm^{-1} (CH_3 C−H stretch), 2223 cm^{-1} (C′N); ^{1}H NMR (300 MHz, $CDCl_3$-*d*, *δ*, ppm) 2.33 (s, 6H, CH_3), 6.91 (d, 2H, H_d), 6.99 (d, 2H, H_c), 7.03 (d, 4H, H_e), 7.09∼7.14 (m, 8H, H_b + H_f), 7.52 (d, 4H, H_a); ^{13}C NMR (75 MHz, $CDCl_3$-*d*, *δ*, ppm) 20.8 (CH_3), 105.3 (C^1), 119.1 (CN), 122.3 (C^3), 122.5 (C^6), 125.1 (C^{10}), 127.9 (C^7), 130.1 (C^{11}), 133.5 (C^2), 137.2 (C^{12}), 137.2 (C^8), 144.7 (C^9), 147.0 (C^5), 150.2 (C^4).

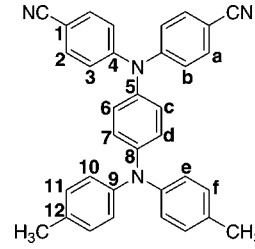

***N,N*-Bis(4-carboxyphenyl)-*N′,N′*-di(4-methylphenyl)-1,4-phenylenediamine (4′).** A mixture of 2.50 g (44 mmol) of potassium hydroxide and 1.31 g (2.67 mmol) of the obtained dinitrile compound (**3′**) in 8 mL of ethanol and 8 mL of distillated water was stirred at about 100 °C until no further ammonia was generated. The time taken to reach this stage was about 5−6 days. The solution was cooled, and the pH value was adjusted by dilute hydrochloric acid to near 3. The yellowish precipitate formed was collected by filtration and washed thoroughly with water. Further purification by recrystallization from acetic acid gave 1.29 g (92% yield) of the pure diacid: mp 327−328 °C measured by DSC at 10 °C/min; IR (KBr) 2700−3400 cm^{-1} (O−H stretch), 1681 cm^{-1} (C═O stretch); ^{1}H NMR (300 MHz, DMSO-d_6, *δ*, ppm) 2.23 (s, 6H, CH_3), 6.88 (d, 2H, H_d), 6.95 (d, 4H, H_e), 6.98 (d, 2H, H_c), 7.04 (d, 4H, H_b), 7.10 (d, 4H, H_f), 7.83 (d, 4H, H_a), 12.67 (s, 2H, COOH); ^{13}C NMR (75 MHz, DMSO-d_6, *δ*, ppm) 20.6 (CH_3), 121.7 (C^3), 122.8 (C^7), 124.4 (C^1), 124.8 (C^{10}), 128.1 (C^6), 130.4 (C^{11}), 131.2 (C^2), 132.8 (C^{12}), 138.7 (C^8), 144.7 (C^9), 145.6 (C^5), 150.6 (C^4), 167.0 (C═O). Anal. Calcd for $C_{34}H_{28}N_2O_4$ (528.60): C, 77.25; H, 5.34; N, 5.30. Found: C, 77.07; H, 5.37; N, 5.23.

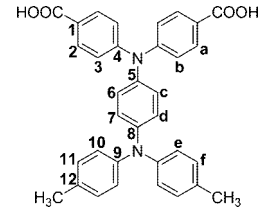

4,4′-Dimethyltriphenylamine (M1). According to known chemistry,[18] compound **M1** (yield 30%, mp 168−170 °C) was prepared by potassium carbonate-mediated aromatic nucleophilic substitution reaction of aniline with 4-iodotoluene. ^{1}H NMR (300 MHz, DMSO-d_6, *δ*, ppm) 2.18 (s, 6H, CH_3), 6.78−7.05 (m, 11H, Ar), 7.16 (t, 2H, Ar); ^{13}C NMR (75 MHz, DMSO-d_6, *δ*, ppm) 20.6 (CH_3), 122.1, 122.6, 124.4, 129.6, 130.3, 132.4, 145.1, 148.0.

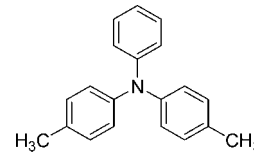

4,4′-Diamidetriphenylamine (M2). A mixture of 0.275 g (1.00 mmol) of 4,4′-diaminetriphenylamine, 0.256 g (2.10 mmol) of benzoic acid,, 1.00 mL of TPP, 0.5 mL of Py, and 1.00 mL of NMP was heated with stirring at 105 °C for 3 h. The mixture was poured slowly into

Table 3. Optical and Electrochemical Properties of Polyamides

	solution λ (nm)[a]				film λ (nm)			oxidation (V) vs Ag/AgCl in CH_3CN						E_{onset}	
index	abs max	PL max	Φ_F[b] (%)	λ_0[c]	abs max	abs onset[d]	PL max[e]	first $E_{1/2}$	first E_{onset}	second $E_{1/2}$	third $E_{1/2}$	fourth $E_{1/2}$	E_g[f] (eV)	HOMO[g] (eV)	LUMO[h] (eV)
Ia	308 (360)[e]	468	0.11	522	313[e] (379)	483		0.59	0.48	0.97	[i]	[i]	2.57	4.84	2.27
Ib	304 (350)[e]	471	0.11	465	308[e] (348)	422	[i]	0.58	0.48	0.96	[i]	[i]	2.94	4.84	1.90
Ic	306 (352)[e]	463	0.12	466	316[e] (356)	435	[i]	0.61	0.49	0.98	[i]	[i]	2.85	4.85	2.00
I′b	(347)[e]	461	0.28	446	(347)[e]	415	[i]	0.63	0.53	1.00	[i]	[i]	2.99	4.89	1.90
IIa	279 (360)[e]	510	0.78	459	317 (361)[e]	447	530	0.73	0.63	1.12	[i]	[i]	2.77	4.99	2.22
IIb	280 (349)[e]	514	0.69	453	313 (358)[e]	442	514	0.76	0.64	1.12	[i]	[i]	2.81	5.00	2.19
IIc	278 (358)[e]	518	0.16	488	(346)[e]	468	[i]	0.58	0.45	0.76	0.96	1.12	2.65	4.81	2.16

[a] Polymer concentration was 10^{-5} mol/L in NMP. The values in parentheses are shoulder band absorbances for solid and solution state. [b] Quantum yield in dilute solution was calculated in an integrating sphere with quinine sulfate as the standard ($\Phi_F = 0.546$). [c] Cutoff wavelength from UV−vis transmission spectra of polymer films (thickness 38∼64 μm). [d] Onset of absorbance from UV−vis absorbance spectra of polymer thin films (thickness 2−5 μm). [e] Excitation wavelengths for solid and solution state. [f] Data were calculated by the equation gap = $1240/\lambda_{onset}$ of polymer film. [g] HOMO energy levels were calculated from cyclic voltammetry and were referenced to ferrocene (4.8 eV). [h] LUMO = HOMO − E_g. [i] No discernible λ_{PL} or half-potential was observed.

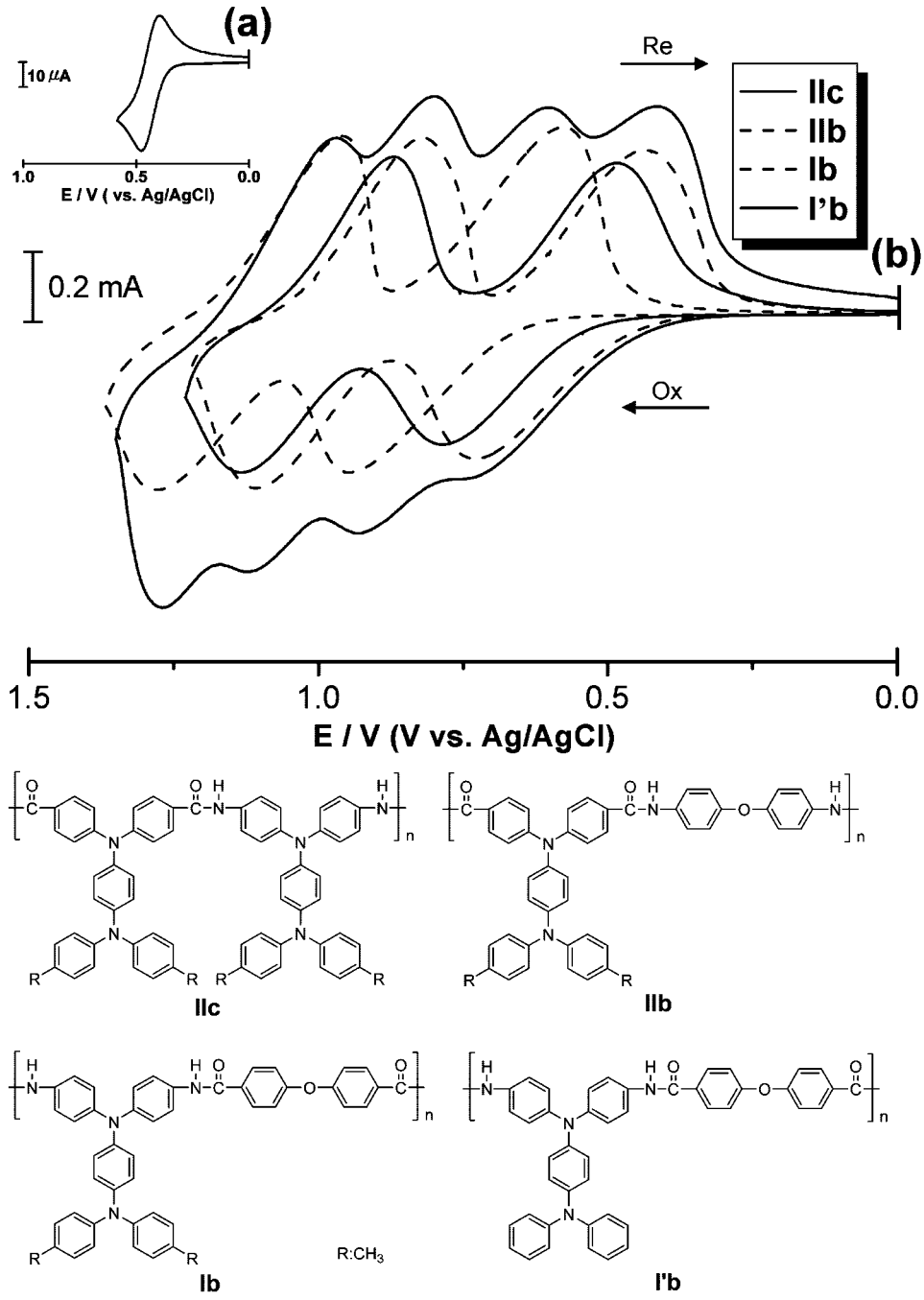

Figure 5. Cyclic voltammograms of (a) ferrocene and (b) polyamides **IIc**, **IIb**, **Ib**, and **I′b** in CH_3CN containing 0.1 M TBAP at scan rate = 0.05 V/s.

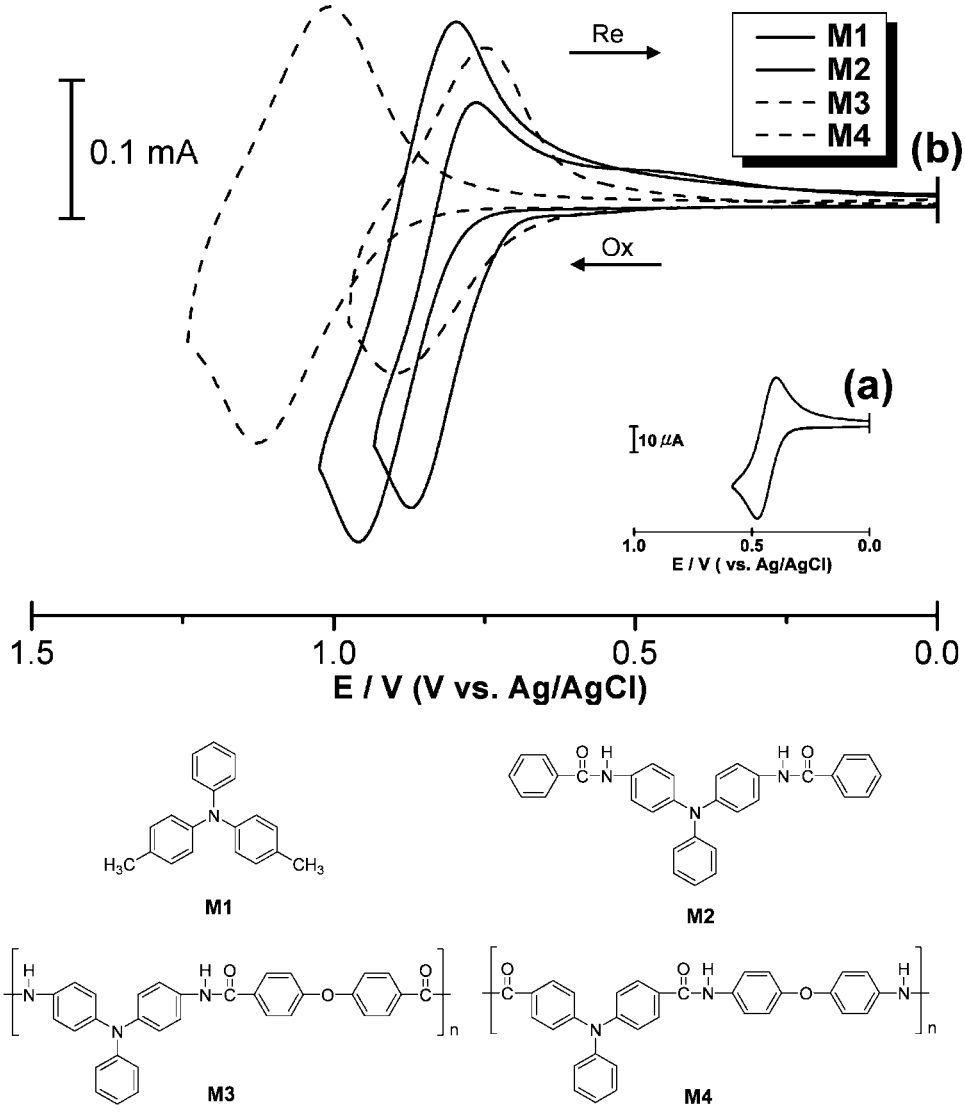

Figure 6. Cyclic voltammograms of (a) ferrocene and (b) model compounds **M1** and **M2** and polyamides **M3** and **M4** in CH_3CN containing 0.1 M TBAP at scan rate = 0.05 V/s.

Table 4. Electrochemical Properties of Model Compounds M1 and M2 and Polyamides M3 and M4

	oxidation potential (V) vs Ag/AgCl in CH_3CN	
index	first $E_{1/2}$	first E_{onset}
M1	0.88	0.80
M2	0.82	0.73
M3	0.82	0.68
M4	1.07	0.90

50 mL of stirring methanol, washed, collected by filtration, and dried under vacuum at 100 °C: yield 0.459 g (95%); ^{1}H NMR (300 MHz, DMSO-d_6, δ, ppm) 6.95−7.03 (m, 7H, Ar), 7.26 (t, 2H, Ar), 7.49−7.58 (m, 6H, Ar), 7.74 (d, 4H, Ar), 7.93 (d, 4H, Ar);^{13}C NMR (75 MHz, DMSO-d_6, δ, ppm) 121.9, 122.1, 122.4, 124.5, 127.8, 128.5, 129.5, 131.6, 134.7, 135.2, 143.2, 147.8, 165.5.

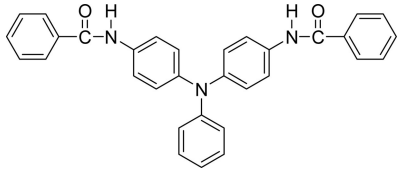

Polymer Synthesis. The synthesis of polyamide **Ib** is used as an example to illustrate the general synthetic route. The typical procedure

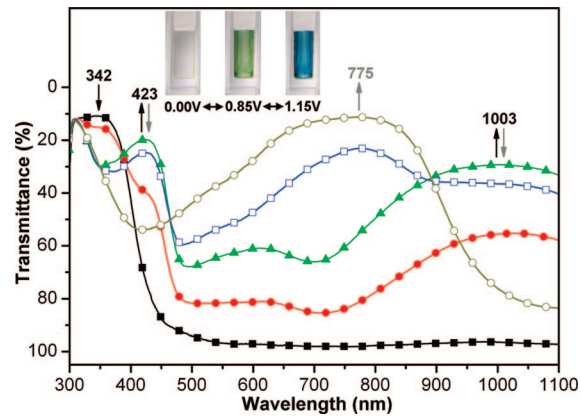

Figure 7. Electrochromic behavior of polyamide **Ib** thin film (in CH_3CN with 0.1 M TBAP as the supporting electrolyte) at (■) 0.00, (●) 0.75, (▲) 0.85, (□) 0.95, and (○) 1.15 V vs Ag/AgCl. $\mathbf{Ib}^{+\bullet}$, solid symbols with black arrows; $\mathbf{Ib}^{2+}$, open symbols with gray arrows.

was as follows. A mixture of 0.470 g (1.00 mmol) of *N*,*N*-bis(4-aminophenyl)-*N*′,*N*′-di(4-methylphenyl)-1,4-phenylenediamine (**4**), 0.258 g (1.00 mmol) of 4,4′-oxybis(benzoic acid) (**5b**), 0.12 g of calcium chloride, 1.00 mL of TPP, 0.5 mL of Py, and 1.00 mL of NMP was heated with stirring at 105 °C for 3 h. The polymer solution was poured

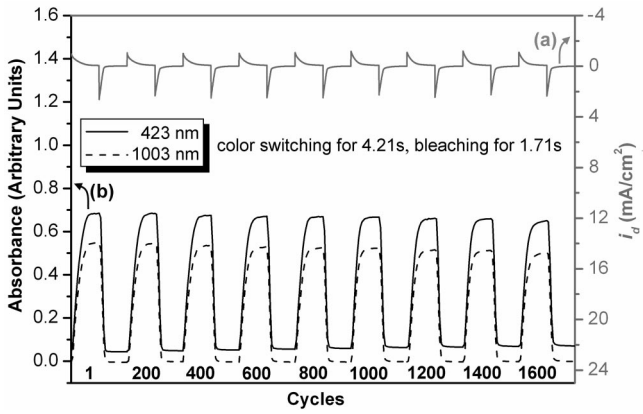

Figure 8. (a) Current consumption and (b) potential step absorptometry of polyamide **Ib** (in CH_3CN with 0.1 M TBAP as the supporting electrolyte) by applying a potential step (0.00 V ⇆ 0.78 V; coated area 1 cm^2) and cycle time 18 s for coloration efficiency from 276 cm^2/C (first cycle) to 253 cm^2/C (1600th cycle).

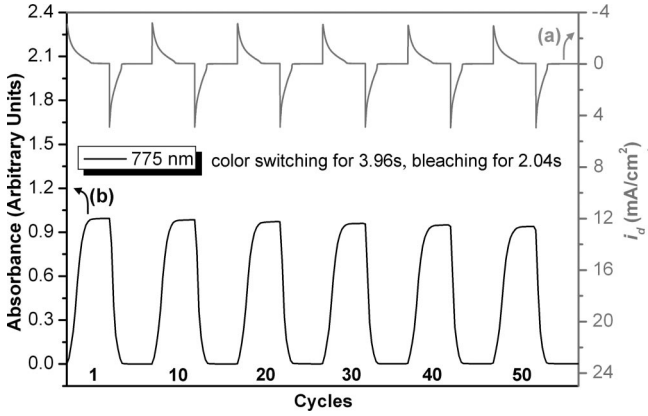

Figure 9. (a) Current consumption and (b) potential step absorptometry of polyamide **Ib** (in CH_3CN with 0.1 M TBAP as the supporting electrolyte) by applying a potential step (0.00 V ⇆ 1.18 V; coated area 1 cm^2) and cycle time 20 s for coloration efficiency from 174 cm^2/C (first cycle) to 172 cm^2/C (50th cycle).

Table 5. Optical and Electrochemical Data Collected for Coloration Efficiency Measurements of Polyamide Ib

cycles[a]	ΔOD_{426}[b]	Q[c] (mC/cm^2)	η[d] (cm^2/C)	decay[e] (%)
1	0.640	2.32	276	0
200	0.635	2.33	273	1.1
400	0.623	2.32	269	2.5
600	0.614	2.31	266	3.6
800	0.610	2.31	264	4.3
1000	0.604	2.31	261	5.4
1200	0.593	2.30	258	6.5
1400	0.591	2.30	257	6.9
1600	0.580	2.29	253	8.3

[a] Times of cyclic scan by applying potential steps: 0.00 ↔ 0.78 for **Ib** (volts vs Ag/AgCl). [b] Optical density change at 426 nm for **Ib**. [c] Ejected charge, determined from in situ experiments. [d] Coloration efficiency is derived from the equation $\eta = \Delta OD/Q$. [e] Decay of coloration efficiency after cyclic scans.

slowly into 300 mL of stirring methanol, giving rise to a stringy, fiberlike precipitate that was collected by filtration, washed thoroughly with hot water and methanol, and dried under vacuum at 100 °C: yield 0.685 g (99%). Reprecipitations from DMAc into methanol were carried out twice for further purification. The inherent viscosity of the obtained polyamide **Ib** was 0.80 dL/g, measured at a concentration of 0.5 g/dL in NMP at 30 °C. The IR spectrum of **Ib** (film) exhibited characteristic amide absorption bands at 3275 cm^{-1} (N−H stretch), 3034 cm^{-1} (aromatic C−H stretch), 2920, 2856 cm^{-1} (CH_3 C−H stretch), and 1643 cm^{-1} (amide carbonyl). The other polyamides were prepared by an analogous procedure.

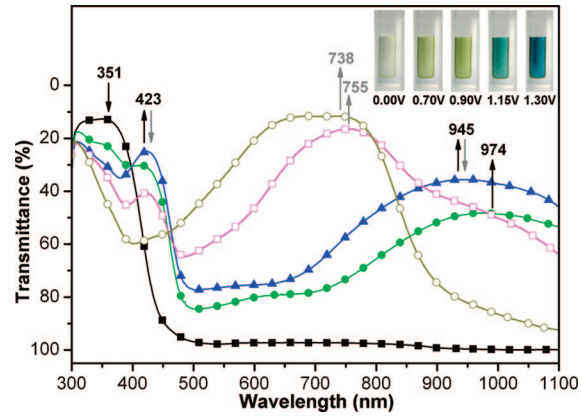

Figure 10. Electrochromic behavior of polyamide **IIc** thin film (in CH_3CN with 0.1 M TBAP as the supporting electrolyte) at (■) 0.00, (●) 0.70, (▲) 0.90, (□) 1.15, and (○) 1.30 V vs Ag/Ag$^+$. **IIc**$^+$ and **IIc**$^{2+}$, solid symbols with black arrows; **IIc**$^{3+}$ and **IIc**$^{4+}$, open symbols with gray arrows.

Preparation of Films. A solution of the polymer was made by dissolving about 0.50 g of the polyamide sample in 10 mL of DMAc or NMP. The homogeneous solution was poured into a 9-cm glass Petri dish, which was placed in a 90 °C oven for 3 h to remove most of the solvent; then the semidried film was further dried in vacuo at 170 °C for 8 h. The obtained films were about 38−64 μm thick and were used for solubility tests and thermal analyses.

Measurements. Infrared spectra were recorded on a Perkin-Elmer RXI FT-IR spectrometer. Elemental analyses were run in an Elementar Vario EL-III. ^{1}H and ^{13}C NMR spectra were measured on a Bruker AV-300 FT-NMR system, and referenced to the $CDCl_3$-d_1 and DMSO-d_6 signals, and peak multiplicity was reported as follows: s, singlet; d, doublet; t, triplet; m, multiplet. The inherent viscosities were determined at 0.5 g/dL concentration on a Tamson TV-2000 viscometer at 30 °C. Wide-angle X-ray diffraction (WAXD) measurements were performed at room temperature (ca. 25 °C) on a Shimadzu XRD-7000 X-ray diffractometer (40 kV, 20 mA), using graphite-monochromatized Cu Kα radiation. Ultraviolet−visible (UV−vis) spectra of the polymers were recorded on a Varian Cary 50 Probe spectrometer. Thermogravimetric analysis (TGA) was conducted with a Perkin-Elmer Pyris 1 TGA. Experiments were carried out on approximately 4−6 mg film samples heated in flowing nitrogen or air (flow rate = 30 cm^3/min) at a heating rate of 20 °C/min. Thermomechanical analysis (TMA) was conducted with a Perkin-Elmer TMA 7 instrument. The TMA experiments were conducted from 50 to 350 °C at a scan rate of 10 °C/min with a penetration probe 1.0 mm in diameter under an applied constant load of 50 mN. Softening temperatures (T_s) were taken as the onset temperatures of probe displacement on the TMA traces. Cyclic voltammetry was performed with a Bioanalytical System model CV-27 potentiostat and a BAS X-Y recorder with ITO (polymer film area about 0.7 cm × 0.7 cm) was used as a working electrode and a platinum wire as an auxiliary electrode at a scan rate of 50 mV/s against a Ag/AgCl reference electrode in a solution of 0.1 M tetrabutylammonium perchlorate (TBAP)/acetonitrile (CH_3CN). Voltammograms are presented with the positive potential pointing to the left and with increasing anodic currents pointing downward. The spectroelectrochemical cell was composed of a 1 cm cuvette, ITO as a working electrode, a platinum wire as an auxiliary electrode, and a Ag/AgCl reference electrode. Absorption spectra in spectroelectrochemical analysis were measured with a HP 8453 UV−visible spectrophotometer. Photoluminescence spectra were measured with a Jasco FP-6300 spectrofluorometer. Fluorescence quantum yields (Φ_F) values of the samples in NMP were measured with quinine sulfate in 1 N H_2SO_4 as a reference standard (Φ_F = 0.546).[19,20] All corrected fluorescence excitation spectra were found to be equivalent to their respective absorption spectra.

Scheme 3. Simplified Redox Process of Polyamide IIc from its Neutral State, Radical Cation State to Dication, Trication, and Tetracation States

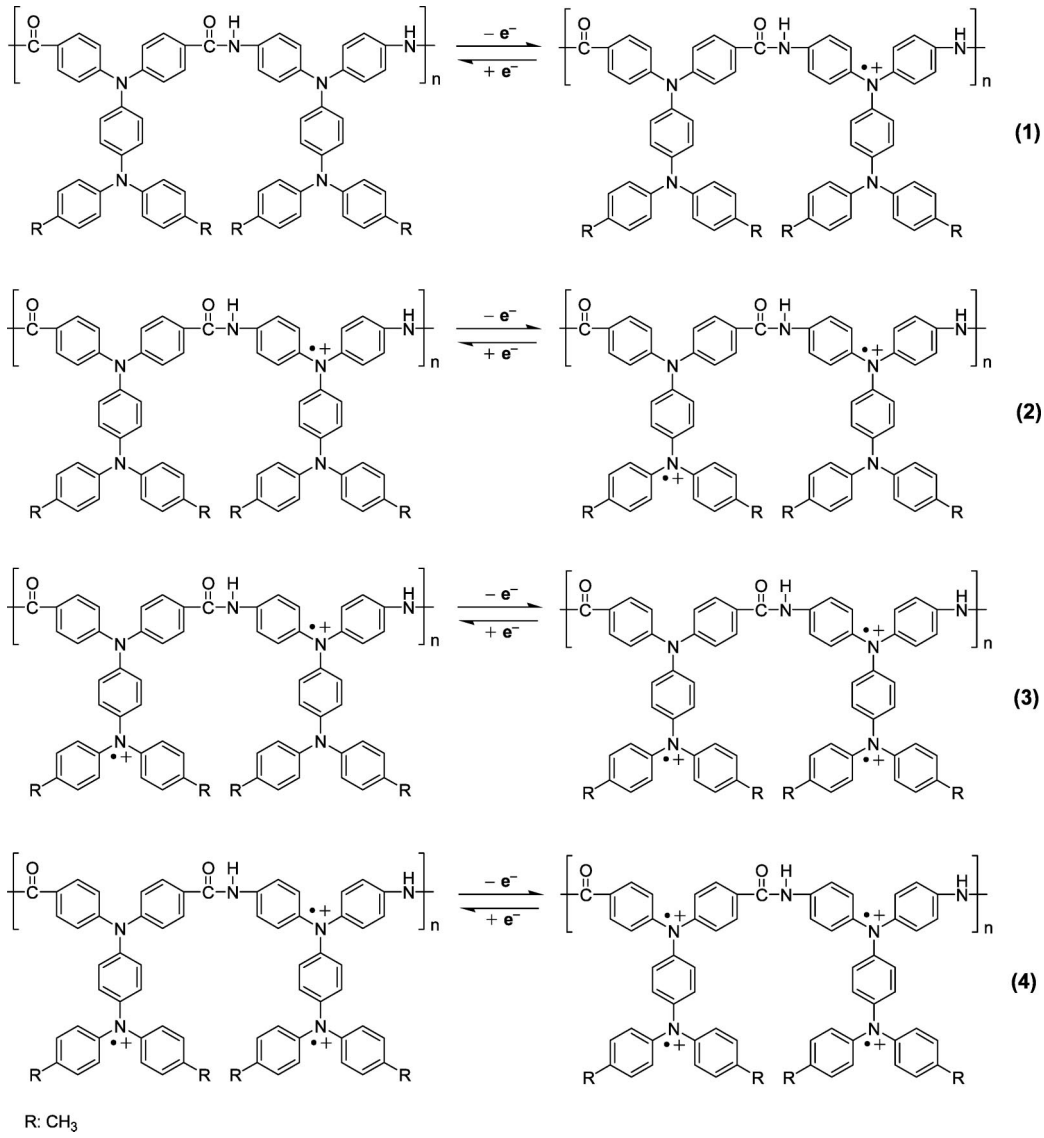

Results and Discussion

Monomer Synthesis. 4-Amino-4′,4″-dimethyltriphenylamine (**2**) was prepared by potassium carbonate-mediated aromatic nucleophilic substitution reaction of 4-nitroaniline with 4-iodotoluene[18] followed by hydrazine Pd/C-catalytic reduction according to the synthetic route outlined in Scheme 1. The new aromatic diamine, *N*,*N*-bis(4-aminophenyl)-*N*′,*N*′-di(4-methylphenyl)-1,4-phenylenediamine (**4**), was successfully synthesized by hydrazine Pd/C-catalyzed reduction of the dinitro compound (**3**) resulting from double N-arylation reaction of compound **2** with 4-fluoronitrobenzene in the presence of cesium fluoride. The new aromatic dicarboxylic acid, *N*,*N*-bis(4-carboxyphenyl)-*N*′,*N*′-di(4-methylphenyl)-1,4-phenylenediamine (**4′**), was also successfully prepared by alkaline hydrolysis of the dinitrile compound (**3′**) resulting from double-coupling reaction of the conjugate base of **2** (1.0 equiv) with 4-fluorobenzonitrile (2.1 equiv). Elemental analysis, IR, and ^{1}H and ^{13}C NMR spectroscopic techniques were used to identify structures of the target compounds **4** and **4′**. The nitro groups of compound **3** gave two characteristic bands at around 1589 and 1316 cm^{-1} (-NO_2 asymmetric and symmetric stretching). After reduction, the characteristic absorptions of the nitro group disappeared, and the amino group showed the typical N−H stretching absorption pair in the region of 3300−3500 cm^{-1}. Figure 1 illustrates the ^{1}H and ^{13}C NMR spectra of the diamine monomer **4**. The ^{1}H NMR spectrum confirms that the nitro groups have been completely transformed into amino groups by the high-field shift of the aromatic protons and the resonance signals at around 4.93 ppm corresponding to the amino protons. The IR spectra of dinitrile compound **3′** gave a characteristic sharp band at 2223 cm^{-1} peculiar to the cyano group. After hydrolysis, the characteristic absorption of the cyano group disappeared, and the carboxylic acid group showed a typical carbonyl absorption band at 1681 cm^{-1} (C═O stretching) together with the appearance of broad bands around 3400−2700 cm^{-1} (O−H stretching). Figure 2 exhibits the ^{1}H and ^{13}C NMR spectra of compound **4′**. The ^{13}C NMR spectrum confirms that the cyano groups were completely converted into carboxylic acid groups by the disappearance of the resonance peak for cyano carbon at 119.1 ppm and the appearance of the carbonyl peak at 167.0 ppm. Other important evidence of this change is the shifting of the carbon resonance signals of C^1 adjacent to the cyano or carboxyl group. The C^1 carbons of dinitrile **3′** resonated at a higher field (105.3 ppm) than the other aromatic carbons because of anisotropic shielding by the π electrons of C≡N. After hydrolysis, the resonance peak of C^1 shifted to a

lower field (124.4 ppm) because of the lack of an anisotropic field.

Polymer Synthesis. According to the phosphorylation technique first described by Yamazaki et al.,[21,22] two series of novel polyamides **I** and **II** with pendent 4,4′-dimethyl-substituted triphenylamine units were synthesized from diamine **4** with various dicarboxylic acids, and from dicarboxylic acid **4′** with various diamines, via solution polycondensation with TPP and Py as condensing agents as shown in Scheme 2. All the polymerizations proceeded homogeneously throughout the reaction and afforded clear and highly viscous polymer solutions, which precipitated in a tough, fiberlike form when the resulting polymer solutions were slowly poured into stirring methanol. As shown in Table 1, the obtained polyamides had inherent viscosities in the range of 0.34−0.80 dL/g and could be solution-cast into flexible and tough films, indicating the formation of high molecular weight polymers.

The formation of polyamides was also confirmed by IR and NMR spectroscopy. Figure 3 shows a typical IR spectrum for polyamide **Ib**. The characteristic IR absorption bands of the amide group were around 3275 (N−H stretching) and 1643 cm^{-1} (amide carbonyl).

Basic Characterization. The solubility behavior of polyamides was tested qualitatively, and the results are summarized in Table 1. All the polyamides were highly soluble in polar solvents such as NMP and DMAc. The enhanced solubility could be attributed to introduction of the bulky pendent 4,4′-dimethyl-substituted TPA moiety into the repeat unit. Thus, the excellent solubility makes these polymers potential candidates for practical applications by spin- or dip-coating processes.

Wide-angle X-ray diffraction (WAXD) patterns of the polyamides in Figure 4 indicate that the polymers were essentially amorphous, revealing that the 4,4′-dimethyl-substituted TPA-containing polyamides do not form a well-packed structure. The amorphous nature of these polyamides was reflected not only in their good solubility but also in the UV−vis data of the polymers. The UV−vis absorption peaks of the polymers do not shift from the solutions to the films, implying that there is no significant $\pi-\pi$ interaction aggregation between the polymer chains.

Thermal properties of the polyamides were investigated by TGA and TMA. The results are summarized in Table 2. All the aromatic polyamides exhibited good thermal stability with insignificant weight loss up to 450 °C in nitrogen. Their 10% weight-loss temperatures in nitrogen and air were recorded at 540−555 and 505−545 °C, respectively. The carbonized residue (char yield) of these aromatic polymers was more than 68% at 800 °C in nitrogen atmosphere. The high char yields of these polymers could be ascribed to their high aromatic content. The softening temperature (T_s) values of the polymer films were determined from the onset temperature of the probe displacement on the TMA trace.

Optical and Electrochemical Properties. Optical and electrochemical properties of the polyamides were investigated by UV−vis and photoluminescence spectroscopy and by cyclic voltammetry. The results are summarized in Table 3. The UV−vis absorption of these polymers exhibited strong absorption at 278−360 nm in NMP solutions, which are assignable to a $\pi-\pi^*$ transition resulting from conjugation between the aromatic rings and nitrogen atoms. The UV−vis absorption of 4,4′-dimethyl-substituted TPA-based polyamide films **Ia**−**IIc** also showed similar absorbance at 308−379 nm. Aromatic polyamides **Ia**−**IIc** in NMP exhibited fluorescence emission maxima at 463−518 nm with quantum yields ranging from 0.11% to 0.78%. The cutoff wavelengths (absorption edge) from UV−vis transmittance spectra were in the range 453−522 nm.

Electrochemical behavior of the polyamides **I** and **II** series was investigated by cyclic voltammetry conducted by film cast on an ITO-coated glass substrate as the working electrode in dry acetonitrile (CH_3CN) containing 0.1 M TBAP as an electrolyte under nitrogen atmosphere. The typical cyclic voltammograms for polyamides **IIc, IIb, Ib** (with 4,4′-dimethyl-substituted) and **I′b** (without 4,4′-dimethyl-substituted) are shown in Figure 5 for comparison. There are two reversible oxidation redox couples at $E_{1/2}$ values of 0.58 (E_{onset} = 0.48) and 0.96 V for polyamide **Ib**, and 0.63 (E_{onset} = 0.53) and 1.00 V for polyamide **I′b** in the oxidative scan. Polymer **IIc** has four reversible oxidation redox couples at $E_{1/2}$ = 0.58, 0.76, 0.96, and 1.12 V corresponding to successive one-electron removal from the nitrogen atoms at both *N*,*N*,*N*′,*N*′-tetraphenyl-1,4-phenylenediamine structures in each repeating unit to yield two stable delocalized radical cations, polyamide^{+} and polyamide^{3+}, and two stable quinonoid-type dications, polyamide^{2+} and polyamide^{4+}.[23] Because of the electrochemical stability and good adhesion between the polymer film and ITO substrate, polyamide **Ib** exhibited excellent reversibility of electrochromic characteristics by continuous 3000 cyclic scans between 0.0 and 0.78 V with changes from colorless to green. Comparing the electrochemical data, we found that polyamide **Ib** was more easily oxidized than polyamide **I′b** (0.58 vs 0.63 V). Figure 6 indicates electrochemical behavior for model compounds **M1** and **M2** and polyamides **M3** and **M4**; they have reversible oxidation redox couples at $E_{1/2}$ = 0.88 (E_{onset} = 0.80), 0.82 (E_{onset} = 0.73), 0.82 (E_{onset} = 0.68), and 1.07 (E_{onset} = 0.90), respectively, to prove the oxidation order of nitrogen atoms for polyamide **IIc** according to the electron density among the four nitrogen atoms on different *p*-phenylenediamine structures in each repeating unit, and the results are summarized in Table 4. From these electrochemical data, the first electron removal for polyamide **Ib** could be assumed to occur at the N atom on the main-chain triphenylamine unit, which was more electron-rich than the N atom on the pendent 4,4′-dimethyltriphenylamine groups. The introduction of electron-donating 4,4′-dimethyltriphenylamine not only largely prevents the coupling reaction but also lowers the oxidation potentials of the electroactive polyamides **I** when compared with the corresponding polyamides **I′** without methyl substituent. The mechanism of these phenomena also agreed with the results from the corresponding polymers with *p*-methoxy groups.[9b,c] The energy of the highest occupied molecular orbital (HOMO) and lowest unoccupied molecular orbital (LUMO) levels of the investigated polyamides could be determined from the oxidation onset potentials and the onset absorption wavelength of polymer films, and the results are listed in Table 3. For example (Figure 5), the oxidation half-wave potential for polyamide **Ib** was determined to be 0.58 V (E_{onset} = 0.48 V) versus Ag/AgCl. The external ferrocene/ferrocenium (Fc/Fc^+) redox standard E_{onset} (Fc/Fc^+) was 0.44 V versus Ag/AgCl in CH_3CN. Under the assumption that the HOMO energy for the Fc/Fc^+ standard was 4.80 eV with respect to the zero vacuum level, the HOMO energy for polyamide **Ib** was evaluated to be 4.84 eV.

Electrochromic Characteristics. Electrochromism of the polyamides thin films was examined by an optically transparent thin-layer electrode (OTTLE) coupled with UV−vis spectroscopy. The electrode preparations and solution conditions were identical to those used in cyclic voltammetry. All these polyamides exhibited similar electrochromic properties, and the typical electrochromic transmittance spectrum of polyamide **Ib** is shown in Figure 7. When the applied potentials increased positively from 0 to 0.85 V, the peak of transmittance at 342 nm, characteristic for neutral-form polyamide **Ib**, decreased gradually. Two new bands grew up at 423 and 1003 nm due to the first-stage oxidation. When the potential was adjusted to a

more positive value of 1.15 V, corresponding to the second-step oxidation, the peak of characteristic absorbance decreased gradually and one new band grew up at 775 nm. Meanwhile, the film changed from original colorless to green and then to a blue oxidized form. Polymer **Ib** exhibited high contrast of optical transmittance change (ΔT, %) up to 52% at 423 nm and 67% at 1003 nm for green, and 87% at 775 nm for blue (as shown in Figure 7).

The color switching times were estimated by applying a potential step, and the absorbance profiles were followed (Figures 8 and 9 for **Ib**). The switching time was defined as the time required to reach 90% of the full change in absorbance after the switching of the potential. Thin film from polyamide **Ib** required 4.21 s at 0.78 V for switching absorbance at 423 and 1003 nm and 1.71 s for bleaching. When the potential was set at 1.18 V, thin film **Ib** required 3.96 s for coloration at 775 nm and 2.04 s for bleaching. After over 1600 cyclic switches for green color, the films of polyamide **Ib** showed excellent continuous cyclic stability of electrochromism. The high electrochromic coloration efficiency of green ($\eta = \Delta OD_{423}/Q$) (276 cm^2/C for 1 cycle to 253 cm^2/C for 1600 cycles) and blue ($\eta = \Delta OD_{775}/Q$) (174 cm^2/C for 1 cycle to 172 cm^2/C for 50 cycles) of polyamide **Ib** and decay of polyamide **Ib** were also calculated,[24] and the results are summarized in Table 5.

The multiple-color electrochromic absorption spectrum of polyamide **IIc** is shown in Figure 10. When the applied potentials increased positively from 0 to 0.70, 0.90, 1.15, and 1.30 V, respectively, corresponding to the first, second, third, and fourth electron oxidation, the peak of characteristic absorbance at 351 nm for neutral-form polyamide **IIc** decreased gradually, while four new bands grew up at 974, 945, 755, and 738 nm, respectively. The new spectral patterns were assigned as those of the cationic radical polyamide^{+}, polyamide^{2+}, polyamide^{3+}, and polyamide^{4+}, respectively, which are the products obtained by electron removal from the lone pair of the nitrogen atom on different two *p*-phenylenediamine structures. According to the electron density among the four nitrogen atoms on two different *p*-phenylenediamine structures in each repeating unit, the anodic oxidation pathway of polyamide **IIc** was postulated as in Scheme 3.

Conclusions

Two series of highly stable anodic green and blue electrochromic polyamides with high contrast of optical transmittance change (ΔT, %) up to 52% at 423 nm and 67% at 1003 nm for green and 87% at 775 nm for blue have been readily prepared from the new, structurally similar diamine (**4**) and diacid (**4′**) via direct phosphorylation polycondensation. By incorporating electron-donating methyl substituents at the para position of *N*,*N*,*N*′,*N*′-tetraphenyl-1,4-phenylenediamine, not only were the oxidation potentials of the electroactive polyamides lowered, but also this could be a good approach to facile color tuning of the electrochromic behaviors due to the different multistage oxidation potentials. In addition to the enhanced solubility and excellent thin film formability, these novel aromatic polyamides also showed excellent continuous cyclic stability of anodic polyelectrochromic characteristic with good coloration efficiency of green (276 cm^2/C for 1 cycle to 253 cm^2/C for 1600 cycles) and blue (174 cm^2/C for 1 cycle to 172 cm^2/C for 50 cycles). The color changes from the colorless or pale yellowish neutral form to the green form when scanning potentials change positively from 0.00 to 0.78 V. After over 1600 cyclic switches, the polymer films still exhibited excellent reversibility of electrochromic characteristics. Thus, the 4,4′-dimethyl-substituted TPA-based polyamides could be good candidates for anodic electrochromic materials due to their proper oxidation potentials, excellent electrochemical stability, and thin film formability.

Acknowledgment. We are grateful to the National Science Council of the Republic of China for financial support of this work.

References and Notes

(1) (a) Monk, P. M. S.; Mortimer, R. J.; Rosseinsky, D. R. *Electrochromism: Fundamentals and Applications*; VCH: Weinheim, Germany, 1995. (b) Monk, P. M. S.; Mortimer, R. J.; Rosseinsky, D. R. *Electrochromism and Electrochromic Devices*; Cambridge University Press: Cambridge, U.K., 2007.
(2) Kido, J.; Kimura, M.; Nagai, K. *Science* **1995**, *267*, 1332.
(3) Brotherston, I. D.; Mudigonda, D. S. K.; Osbron, J. M.; Belk, J.; Chen, J.; Loveday, D. C.; Boehme, J. L.; Ferraris, J. P.; Meeker, D. L. *Electrochim. Acta* **1999**, *44*, 2993.
(4) Schwendeman, I.; Hwang, J.; Welsh, D. M.; Tanner, D. B.; Reynolds, J. R. *Adv. Mater.* **2001**, *13*, 634.
(5) (a) Rosseinsky, D. R.; Mortimer, R. J. *Adv. Mater.* **2001**, *13*, 783. (b) Rauh, R. D. *Electrochim. Acta* **1999**, *44*, 3165. (c) Arbizzani, C.; Mastragostino, M.; Zanelli, A. *Sol. Energy Mater. Sol. Cells* **1995**, *39*, 213.
(6) (a) Reeves, B. D.; Thompson, B. C.; Abboud, K. A.; Smart, B. E.; Reynolds, J. R. *Adv. Mater.* **2002**, *14*, 717. (b) Argun, A. A.; Aubert, P. H.; Thompson, B. C.; Schwendeman, I.; Gaupp, C. L.; Hwang, J.; Pinto, N. J.; Tanner, D. B.; MacDiarmid, A. G.; Reynolds, J. R. *Chem. Mater.* **2004**, *16*, 4401.
(7) (a) Gaupp, C. L.; Reynolds, J. R. *Macromolecules* **2003**, *36*, 6305. (b) Reeves, B. D.; Grenier, C. R. G.; Argun, A. A.; Cirpan, A.; McCarley, T. D.; Reynolds, J. R. *Macromolecules* **2004**, *37*, 7559. (c) Witker, D.; Reynolds, J. R. *Macromolecules* **2005**, *38*, 7636. (d) Thompson, B. C.; Kim, Y.-G.; McCarley, T. D.; Reynolds, J. R. *J. Am. Chem. Soc.* **2006**, *128*, 12714.
(8) (a) Sonmez, G.; Meng, H.; Wudl, F. *Chem. Mater.* **2004**, *16*, 574. (b) Sonmez, G.; Sonmez, H. B.; Shen, C. K. F.; Wudl, F. *Adv. Mater.* **2004**, *16*, 1905. (c) Sonmez, G.; Shen, C. K. F.; Rubin, Y.; Wudl, F. *Angew. Chem., Int. Ed.* **2004**, *43*, 1497. (d) Sonmez, G.; Sonmez, H. B.; Shen, C. K. F.; Jost, R. W.; Rubin, Y.; Wudl, F. *Macromolecules* **2005**, *38*, 669.
(9) (a) Liou, G. S.; Hsiao, S. H.; Su, T. H. *J. Mater. Chem.* **2005**, *15*, 1812. (b) Chang, C. W.; Liou, G. S.; Hsiao, S. H. *J. Mater. Chem.* **2007**, *17*, 1007. (c) Liou, G. S.; Chang, C. W. *Macromolecules* **2008**, *41*, 1667.
(10) Creutz, C.; Taube, H. *J. Am. Chem. Soc.* **1973**, *95*, 1086.
(11) Lambert, C.; Noll, G. *J. Am. Chem. Soc.* **1999**, *121*, 8434.
(12) Leung, M. K.; Chou, M. Y.; Su, Y. O.; Chiang, C. L.; Chen, H. L.; Yang, C. F.; Yang, C. C.; Lin, C. C.; Chen, H. T. *Org. Lett.* **2003**, *5*, 839.
(13) Robin, M.; Day, P. *Adv. Inorg. Radiochem.* **1967**, *10*, 247.
(14) Szeghalmi, A. V.; Erdmann, M.; Engel, V.; Schmitt, M.; Amthor, S.; Kriegisch, V.; Noll, G.; Stahl, R.; Lambert, C.; Leusser, D.; Stalke, D.; Zabel, M.; Popp, J. *J. Am. Chem. Soc.* **2004**, *126*, 7834.
(15) (a) Kumar, A.; Welsh, D. M.; Morvant, M. C.; Piroux, F.; Abboud, K. A.; Reynolds, J. R. *Chem. Mater.* **1998**, *10*, 896. (b) Sapp, S. A.; Sotzing, G. A.; Reynolds, J. R. *Chem. Mater.* **1998**, *10*, 2101. (c) Welsh, D. M.; Kumar, A.; Meijer, E. W.; Reynolds, J. R. *Adv. Mater.* **1999**, *11*, 1379. (d) Schwendeman, I.; Hickman, R.; Sonmez, G.; Schottland, P.; Zong, K.; Welsh, D. M.; Reynolds, J. R. *Chem. Mater.* **2002**, *14*, 3118.
(16) Su, T. H.; Hsiao, S. H.; Liou, G. S. *J. Polym. Sci., Part A: Polym. Chem.* **2005**, *43*, 2085.
(17) Cheng, S. H.; Hsiao, S. H.; Su, T. H.; Liou, G. S. *Macromolecules* **2005**, *38*, 307.
(18) Yano, M.; Ishida, Y.; Aoyama, K.; Tatsumi, M.; Sato, K.; Shiomi, D.; Ichimura, A.; Takui, T. *Synth. Met.* **2003**, *137*, 1275.
(19) (a) Pyo, S. M.; Kim, S. I.; Shin, T. J.; Ree, M.; Park, K. H.; Kang, J. S. *Macromolecules* **1998**, *31*, 4777. (b) Kim, J. S.; Ahn, H. K.; Ree, M. *Tetrahedron Lett.* **2005**, *46*, 277. (c) Pyo, S. M.; Kim, S. I.; Shin, T. J.; Ree, M.; Park, K. H.; Kang, J. S. *Polymer* **1998**, *40*, 125. (d) Shin, T. J.; Park, H. K.; Lee, S. W.; Lee, B.; Oh, W.; Kim, J. S.; Baek, S.; Hwang, Y. T.; Kim, H. C.; Ree, M. *Polym. Eng. Sci.* **2003**, *46*, 1232. (e) Pyo, S. M.; Shin, T. J.; Kim, S. I.; Ree, M. *Mol. Cryst. Liq. Cryst.* **1998**, *316*, 353.
(20) Demas, J. N.; Crosby, G. A. J. *Phys. Chem.* **1971**, *75*, 991.
(21) Yamazaki, N.; Higashi, F.; Kawabata, J. *J. Polym. Sci., Polym. Chem. Ed.* **1974**, *12*, 2149.
(22) Yamazaki, N.; Matsumoto, M.; Higashi, F. *J. Polym. Sci., Polym. Chem. Ed.* **1975**, *13*, 1375.
(23) Selby, T. D.; Kim, K. Y.; Blackstock, S. C. *Chem. Mater.* **2002**, *14*, 1685.
(24) Mortimer, R. J.; Reynolds, J. R. *J. Mater. Chem.* **2005**, *15*, 2226.

MA801227J